J. Membrane Biol. 82, 157–166 (1984)

The Journal of
Membrane Biology

Protoplast Rotation in a Rotating Electric Field: The Influence of Cold Acclimation

Richard V.E. Lovelace†, Darryl G. Stout‡*, and Peter L. Steponkus‡
Department of Applied Physics† and Department of Agronomy‡, Cornell University, Ithaca, New York 14853-0144

Summary. An experimental and theoretical investigation has been made of the rotation of protoplasts of *Secale cereale* L. (cv Puma) in a rotating electric field for the purpose of determining the electrical properties of the protoplast plasma membrane. The dependence of the protoplast rotation rate on: (1) the rotation rate of the applied electric field; (2) the electrical conductivity of the external medium; and (3) cold acclimation or lack thereof were determined. A theoretical analysis of the rotation rate of polarizable spherical cells in a rotating electric field leads to a qualitatively similar formula to that of Arnold and Zimmermann (*Z. Naturforsch.* **37**:908–915, 1982), but it differs from this earlier work by a large numerical factor (~180). Detailed comparisons of the observed protoplast rotation rates with the new theory show generally good agreement. The protoplast rotation measurements allow a noninvasive determination of the specific plasma membrane capacitance, c_m. The average value found in the present experiments is $c_m = (0.56 \pm 0.08) \times 10^{-2}$ F/m². Within the experimental errors, the c_m values are the same for cold-acclimated and noncold-acclimated protoplasts. Determination of plasma membrane resistance from protoplast rotation measurements does not appear feasible because of the high values of the specific resistance.

Key Words Isolated protoplasts · plasma membrane · electrical properties · protoplast rotation · membrane capacitance · cold acclimation

Introduction

Cell and protoplast rotation have been observed in both alternating (Teixeira-Pinto, Nejelski, Cutler & Heller, 1960; Furedi & Ahad, 1964; Pohl & Crane, 1971; Holzapfel, Vienken & Zimmermann, 1982) and rotating electric fields (Arnold & Zimmermann, 1982). In a simple alternating electric field only cells or protoplasts in close proximity to each other exhibit rotation. In contrast, single isolated cells or protoplasts rotate in a rotating electric field. For quantitative studies of protoplast rotation, the use of a rotating electric field has a number of advantages (Arnold & Zimmermann, 1982). An advantage of the rotating field method for the determination of the membrane properties of small cells or protoplasts is that it does not involve a perturbation of the membrane by microelectrode penetration.

Holzapfel et al. (1982) and Arnold and Zimmermann (1982) concluded that protoplast rotation is a result of the induction of a protoplast electric dipole moment because of membrane charging through the resistive suspending solution (Maxwell-Wagner model). The electric dipole moment induced on the protoplast plasma membrane interacts with the rotating electric field causing the protoplast to rotate. The protoplast rotation rate $d\theta_c/dt$ has a characteristic nonmonotonic dependence on the rotation rate of the electric field ω. Arnold and Zimmermann (1982) calculated the specific capacitance of the membrane c_m from the relationship of the (optimum) electric field rotation rate (which gives the maximum $d\theta_c/dt$) and solution conductivity. A value of c_m considered typical for biological membranes was found if it was assumed that the tonoplast and plasma membrane acted as two capacitors in series. Although this estimate of membrane capacitance was considered as evidence supporting the Maxwell-Wagner model, the variability of the measurements was greater than could be accounted for by known sources of error. Lipophilic ions and enzymes such as pronase displace the optimum frequency for rotation (Zimmermann, 1982). Thus, membrane properties other than capacitance may affect protoplast rotation.

The objective of the work reported here was to (a) develop and improve the measurements and the theory of protoplast rotation for the purpose of more accurately deriving the electrical parameters of the protoplast plasma membrane; (b) determine if membrane resistance as well as membrane capacitance could be derived from protoplast rotation

* *Permanent address:* Range Research Station, Agriculture Canada, Kamloops, B.C. V2B 8A9, Canada.

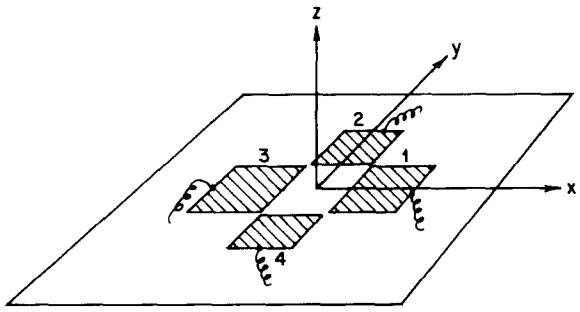

Fig. 1. Diagram of the rotating field chamber

measurements; and (c) to investigate the influence of cold acclimation on protoplast electrical properties.

Materials and Methods

Plant Culture and Protoplast Isolation

Seedlings of *Secale cereale* L. cv. Puma were grown for 7 days in vermiculite in a controlled environment (16-hr light period at 20°C and 8-hr dark period at 15°C). Nonacclimated plants were maintained in this environment for an additional 7 days prior to isolation of protoplasts. Plants to be acclimated were transferred to a 13°C light period (11.5 hr)/7°C dark period (12.5 hr) regime for one week and then transferred to a 2°C (10-hr light period) regime for an additional 4 weeks.

Protoplasts were enzymically isolated from leaves in a solution of 1.5% (wt/vol) cellulysin (Calbiochem), 0.5% macerase (Calbiochem), and 0.3% potassium dextran sulfate as previously described (Wiest & Steponkus, 1978). For the isolation of protoplasts from nonacclimated leaves, 0.5 M sorbitol was used as an osmoticum. Isolation of protoplasts from acclimated leaves required 0.9 M sorbitol as an osmoticum due to the increase in the internal solute concentration during cold acclimation. Protoplasts were washed 3 times in sorbitol and resuspended in a sorbitol plus KCl (0 to 3.0 mM) solution at a final titer of 1.50×10^5 protoplasts/ml. The LT_{50} (temperature at which 50% of the protoplasts survived) was −3 to −5°C for nonacclimated and −25 to −30°C for acclimated protoplasts frozen and thawed in sorbitol solutions.

Chamber Design, Production of the Rotating Electric Field, and Measurement of the Suspending Medium Conductivity

The chamber for subjecting the protoplasts to a rotating electric field (Fig. 1) was constructed using four platinum electrodes (2.0 mm wide × 200 μm thick) set at right angles to each other (*see* Appendix A). The electrodes were fastened to a glass microscope slide with epoxy resin. The central cavity (approximately 2 × 2 × 0.2 mm) of the chamber was then coated with a silicon preparation (Sigmacoate, Sigma Chemicals) to minimize protoplast adherence to the glass slide.

A rotating electric field was produced by applying one sine wave to a pair of opposite electrodes, and a second sine wave, 90° out of phase with the first, to the other pair of opposite electrodes (*see* Appendix A). One electrode of each pair was grounded. The 90° phase shifter was an audio transformer (TRW, D1-T41) with a center-tapped secondary connected to a variable (0 to 10 kΩ) series resistance R–C circuit (Simpson, 1974). The two sine waves were observed with a dual-channel oscilloscope (Telequipment Type D54). At each frequency, R was adjusted to obtain a 90° phase shift. A 250 kΩ potentiometer was connected in series with the output of the unshifted sine wave so that the voltage of the sine waves could be made equal. The shifter and signal generator (General Radio 1310-B Oscillator) combination provided up to 12 volts peak to peak over the frequency range 2 to 450 kHz. One of three different capacitors (27, 10 or 0.860 μF) was switched into the circuit to obtain this frequency range.

The suspending medium conductivity (σ_e) was measured directly on the microscope slide before and after measuring rotation of a protoplast at different electric field rotation rates. The measurements were done at room temperature, $T = 22$°C. A protoplast titer of approximately 2×10^4 protoplasts per ml was used. For these measurements a conductivity meter (YSI Model 31) was connected to one pair of opposite electrodes; the cell constant for these electrodes with a constant volume (27 μl) of solution was determined using KCl standards.

Measurement of Protoplast Rotation

Protoplast rotation was determined with a video image processor (*see* Steponkus et al., 1984). A high-resolution video camera (Hamamatsu C-1000-1) was interfaced to the microscope, and the video image was digitized in real time using a video image array processor (DeAnza Systems Model 6424 VO). The digitized video image (512 × 512 pixels) was displayed on a high-resolution monitor with a hexagonal cursor generated in the video overlay plane. The size and location of the cursor was variable and controlled by a joystick interface. When using a 40× objective and a 10× photo eyepiece, the video image displayed on the monitor corresponded to a 98 × 98 μm field of view. The overlay plane in which the cursor was generated was a 512 × 512 pixel matrix. Thus, the measuring divisions corresponded to approximately 0.19 μm.

For measurement of protoplast rotation (radians/sec), the boundaries of the protoplast image were defined with the hexagonal cursor to establish the radius of the protoplast. Then, using a distinctive feature of the protoplast image as a fiducial mark and intersecting chords of the hexagonal cursor as a reference mark, the rate of rotation was timed using the crystal clock of the image processor computer. A minimum of three successive determinations were made at each electric field rotation frequency.

Measurement of K^+ Concentration

The K^+ content of isolated protoplast suspensions was determined by atomic absorption spectroscopy. Protoplast suspensions (in sorbitol) were frozen and thawed three times in liquid N_2. The suspension was then centrifuged at 5000 × g for 10 min, and the pellet resuspended in an equal volume of water and centrifuged again. The supernatants were combined, and NaCl (1000 μg/ml) was added to reduce ionization of potassium. K^+ concentration of the protoplasts was calculated on the basis of a mean protoplast volume of 21 pl, with the protoplast titer of 10^6/ml.

Theory

The theory of the rotation of single cells in a rotating electric field has been discussed previously by Arnold and Zimmermann (1982). Because our analysis leads to a different formula for the cell rotation, we give the main steps of the calculation here. Figure 2 shows the idealized protoplast geometry considered. The inside radius is r_a, the outside radius is r_b, and the membrane thickness is $\delta = r_b - r_a \ll r_a$. We let $\bar{r} = (r_a + r_b)/2$. The cytoplasm ($r < r_a$) is characterized electrically (in MKS units) by its conductivity σ_i (units of $(\Omega m)^{-1}$) and dielectric constant ε_i (units of F/m). (In vacuo, $\varepsilon = \varepsilon_o = 8.85 \times 10^{-12}$ F/m). The membrane is similarly characterized by σ_m and ε_m. The external medium ($r > r_b$) is characterized by σ_e and ε_e. In general, it is possible that these electrical "constants" depend on the frequency (ω) of the applied electric field. [In particular, at low frequencies, $\omega/2\pi < 200$ Hz, ε_m may become strongly dependent on ω (Coster & Smith, 1977).] The main simplification of the model is that the influence of the vacuole is not included. This is justified for the conditions of interest where $\sigma_i \gg \sigma_e$ (*see* Appendix B).

We want to determine the torque on the protoplast due to an externally generated electric field. The actual electric field inside and outside of the protoplast can be written as $\boldsymbol{E}(\boldsymbol{r},t) = \boldsymbol{E}_o(\boldsymbol{r},t) + \boldsymbol{E}_1(\boldsymbol{r},t)$, where $\boldsymbol{E}_o(\boldsymbol{r},t)$ is the external field component, which would exist in the absence of the protoplast, and $\boldsymbol{E}_1(\boldsymbol{r},t)$ is induced field component due to the protoplast. For a determination of the torque on the protoplast, consider an imaginary spherical surface denoted ∂V just outside of the protoplast. An element of area of this surface is denoted dS and the vector area element is $\boldsymbol{dS} = dS\hat{\boldsymbol{r}}$, where $\hat{\boldsymbol{r}}$ is the outward-pointing unit normal vector to the surface at the given point. The rate of momentum flow into the element $\boldsymbol{dS}$ is $-\underset{\sim}{\boldsymbol{T}} \cdot \boldsymbol{dS}$; thus the rate of angular momentum flow into $\boldsymbol{dS}$ is $-(\boldsymbol{r} \times \underset{\sim}{\boldsymbol{T}}) \cdot \boldsymbol{dS}$, where $\underset{\sim}{\boldsymbol{T}}$ is the Maxwell stress tensor. The torque on the protoplast $\boldsymbol{N}$ is equal to the total rate of angular momentum flow through the surface ∂V:

$$\boldsymbol{N} = -\int_{\partial V} (\boldsymbol{r} \times \underset{\sim}{\boldsymbol{T}}) \cdot \boldsymbol{dS}. \tag{1}$$

Here, $\boldsymbol{r} = x\hat{\boldsymbol{x}} + y\hat{\boldsymbol{y}} + z\hat{\boldsymbol{z}}$ is the position vector (from the center of the protoplast), and $\underset{\sim}{\boldsymbol{T}}$ is the Maxwell stress tensor (Jackson, 1975):

$$T_{ij} = (\tfrac{1}{2})(\boldsymbol{E})^2 [\varepsilon_e - \rho(\partial\varepsilon_e/\partial\rho)_T]\delta_{ij} - \varepsilon_e E_i E_j, \tag{2}$$

with $\varepsilon_e = \varepsilon_e(\rho,T)$ the external medium dielectric constant, with ρ and T the density and temperature,

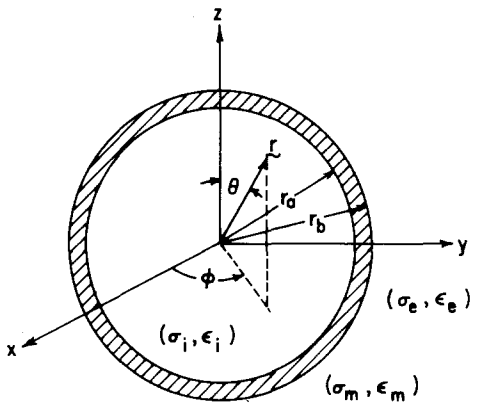

Fig. 2. Diagram of the protoplast geometry assumed in the analysis of the electric fields and currents

and with $\delta_{ij} = 1$ if $i = j$ and $\delta_{ij} = 0$ if $i \neq j$, where i or $j = x,y,z$. Substituting $\boldsymbol{E} = \boldsymbol{E}_o + \boldsymbol{E}_1$ allows the simplification of Eq. (1) to

$$\boldsymbol{N} = \varepsilon_e \int_{\partial V} \boldsymbol{r} \times [E_{oi}E_{1j} + E_{1j}E_{oj}] \cdot dS. \tag{3}$$

That is, only the cross-terms contribute to the torque.

Owing to the small size of the protoplasts investigated ($r_b \cong 13$ to 18 μm), the external field $\boldsymbol{E}_o$ at any given instant is to a good approximation uniform and constant in the vicinity of the protoplast. As discussed in more detail in Appendix B, the induced field outside the protoplast has the form $\boldsymbol{E}_1 = -\nabla\Phi_1$, where

$$\Phi_1 = \boldsymbol{p} \cdot \boldsymbol{r}(4\pi\varepsilon_e r^3)^{-1}, \tag{4}$$

with $\boldsymbol{p}(t)$ the *induced dipole moment* of the protoplast. The evaluation of Eq. (3) gives

$$\boldsymbol{N} = \boldsymbol{p} \times \boldsymbol{E}_o. \tag{5}$$

This formula is well-known in nonpermeable media.

Equation (5) is now used to determine the torque on a protoplast due to a rotating electric field $\boldsymbol{E}_o$. We use the convention that the actual field quantities are given by taking the real part of the complex expressions. An external field rotating counter-clockwise about the z axis is given by $E_x = E_o \exp(-i\omega t)$ and $E_y = iE_o \exp(-i\omega t)$, where for simplicity E_o is taken to be real and where $\omega > 0$. The induced dipole moment is linearly related to E_o; that is, $p_x = \alpha E_o \exp(-i\omega t)$ and $p_y = i\alpha E_o \exp(-i\omega t)$, where the *polarizability* α is derived in Appendix A. Inserting the real parts of $\boldsymbol{p}$ and $\boldsymbol{E}_o$ into Eq. (5) gives

$$N_z = (\boldsymbol{E}_o)^2\, Im(\alpha), \tag{6}$$

with $Im\ (\alpha)$ denoting the imaginary part of α. The details of the calculation of α are given in Appendix B.

The torque of Eq. (6) causes a rotation of the protoplast about the z axis. This rotation is limited by the viscous drag. Because the Reynolds' numbers are much less than unity the viscous drag can be evaluated in the Stokes' flow limit (Landau & Lifshitz, 1959). For a solid sphere uniformly rotating about the z axis at an angular rate of $d\theta_c/dt$ (in radius/s) in an infinite viscous fluid, of dynamic viscosity of η, the drag torque is $N_z^v = -8\pi\eta(\bar{r})^3(d\theta_c/dt)$. For the experimental conditions of interest the protoplast or sphere rests on a solid horizontal plane surface. In this case the drag force can be written as

$$N_z^v = -8\pi g_v g_f \eta(\bar{r})^3(d\theta_c/dt) \tag{7}$$

where $g_v \geq 1$ is a dimensionless factor of the order of unity discussed in Appendix C, and where $g_f \geq 1$ is a further dimensionless factor—the 'friction factor'—assumed to be of order unity introduced to account for any solid body friction between the sphere and the surface.

In the steady state of the rotation of the protoplast, the sum of the torques of Eqs. (6) and (7) is zero. This gives

$$(\boldsymbol{E}_o)^2 Im(\alpha) = 8\pi g_v g_f \eta(\bar{r})^3(d\theta_c/dt). \tag{8}$$

With the approximation discussed in Appendix B, we find

$$\frac{d\theta_c}{dt} = \frac{-3\varepsilon_e(\boldsymbol{E}_o)^2}{4\eta D g_v g_f}\,\frac{f/f_*}{1 + (f/f_*)^2}, \tag{9a}$$

where D is a constant,

$$D \equiv 1 + \frac{2\sigma_e}{\sigma_i} + \frac{1}{2}\left(\frac{R_e}{R_m}\right)\left(1 + \frac{2\sigma_e}{\sigma_i}\right)^2.$$

Here, $f = \omega/2\pi$, and

$$f_* \equiv (2\pi R_m C_m)^{-1} + [\pi R_e C_m(1 + 2\sigma_e/\sigma_i)]^{-1}. \tag{9b}$$

The protoplast membrane resistance is:

$$R_m \equiv \delta[4\pi(\bar{r})^2\sigma_m]^{-1};$$

and its capacitance is:

$$C_m \equiv 4\pi(\bar{r})^2\varepsilon_m(\delta)^{-1}.$$

A characteristic resistance of the external medium is defined as:

$$R_e \equiv (4\pi\bar{r}\sigma_e)^{-1}.$$

In the experiments discussed in this paper, we are in the limit where $\sigma_i \gg \sigma_e$. Consequently,

$$f_* \cong (2\pi R_m C_m)^{-1} + (\pi R_e C_m)^{-1} \tag{10}$$

and

$$D \cong 1 + (\tfrac{1}{2})(R_e/R_m). \tag{11}$$

In most of the subsequent applications of Eq. (9a) we assume $g_v g_f \approx 1$. In Appendix C we show that $g_v \leq 1.222$. In the Discussion section we return to discuss the range of g_f values compatible with our experiments.

It is to be noticed that the minus sign in Eq. (9a) means that *the direction of rotation of the protoplast is opposite to the direction of rotation of the electric field*. This 'counter' rotation can be understood qualitatively by noting that the polarizability α is negative for a very slowly rotating electric field (Appendix B). For a finite rate of rotation of the field, the polarization $\boldsymbol{p}$ of the protoplast does not 'keep up' with the field. That is, the direction of $\boldsymbol{p}$ corresponds to that of $-\boldsymbol{E}$ at a slightly earlier instant. This can be seen to give rise to the counter rotation.

The formula given by Arnold and Zimmermann (1982) is of the form of Eq. (9a). In their formula, however, the vacuum dielectric constant ε_o appears in the numerator of Eq. (9a). Our analysis and observations indicate that the correct factor is $\varepsilon_e = \varepsilon_{re}\varepsilon_o$, with ε_{re} the relative dielectric constant of the external medium. In addition, our equation has a numerical factor of three in the numerator (*see* Appendix B).

Results

The K^+ concentration was calculated to be 70 mM for nonacclimated protoplasts and 190 mM for acclimated protoplasts assuming uniform distribution throughout the protoplast. A 70-mM KCl solution has a conductivity of $8.5 \times 10^{-1}\ (\Omega m)^{-1}$ and a 190 mM KCl solution has a conductivity of $2.14 \times (\Omega m)^{-1}$ (Weast, 1978). The highest suspending medium conductivity used in these experiments was $2.24\ (\pm 12) \times 10^{-2}\ (\Omega m)^{-1}$ for nonacclimated protoplasts and $2.77\ (\pm 12) \times 10^{-2}\ (\Omega m)^{-1}$ for cold-acclimated protoplasts (Table). Therefore, the smallest ratio of σ_i to σ_e was 38 for nonacclimated proto-

Table. Maximum rate of protoplast rotation as a function of suspending solution conductivity

Suspending solution	Solution conductivity[a] ($\times 10^6\ \Omega^{-1}\ cm^{-1}$)	Protoplast radius[a] (μm)	Maximum rate of rotation[a] (rad sec^{-1})	Sample size[b]
Nonacclimated				
0.5 M sorbitol	38 ± 5	14.4 ± 1.9	0.68 ± 0.21	5
0.5 M sorbitol + 0.5 mM KCl	62 ± 7	17.2 ± 1.3	0.62 ± 0.11	4
0.5 M sorbitol + 1 mM KCl	108 ± 4	15.1 ± 1.0	0.51 ± 0.14	5
0.5 M sorbitol + 2 mM KCl	224 ± 12	17.8 ± 1.2	0.47 ± 0.11	3
Cold-acclimated				
0.9 M sorbitol	31 ± 3	14.5 ± 1.2	0.57 ± 0.15	5
0.9 M sorbitol + 0.5 mM KCl	65 ± 3	13.5 ± 1.8	0.78 ± 0.12	5
0.9 M sorbitol + 1 mM KCl	100 ± 1	14.0 ± 0.0	0.56 ± 0.11	3
0.9 M sorbitol + 2 mM KCl	196 ± 8	14.7 ± 2.8	0.50 ± 0.07	2
0.9 M sorbitol + 3 mM KCl	277 ± 12	14.6 ± 0.8	0.43 ± 0.20	4

[a] Values are $x \pm$ SD.

[b] Sample size equals the number of protoplasts measured.

plasts and 77 for cold-acclimated protoplasts. Since $\sigma_i \gg \sigma_e$, the use of Eq. (9a) and Eqs. (10) and (11) is justified.

The protoplast rotation was counter to that of the electric field and the rate $d\theta_c/dt$ was observed to be a maximum at an "optimum" frequency of the applied rotating electric field (Fig. 3) as predicted by the Maxwell-Wagner model (Eq. (9a)). However, the data deviated from that predicted by the model at high and low frequencies. For frequencies significantly higher or lower than the optimum frequency, the protoplast rotation rate exceeded that predicted by the model. Nevertheless, the Maxwell-Wagner model predicts the main dependence of the rotation rate on the frequency of the applied field. For example, the r^2 values shown in Fig. 3 are typical for measurements made on a single protoplast.

The maximum rate of rotation was found to be independent of σ_e (Table). This indicates that the second term of Eq. (11) is approximately zero and that $D = 1$. With $D = 1$, the maximum rate of protoplast rotation was calculated using Eq. (9a). Values for the parameters (η, ε_e and E^2) were estimated as follows. It was assumed that sorbitol and glucose affect viscosity similarly; since the relative viscosity (η/η_o) for 0.5 M glucose is 1.277 and for 0.9 M glucose is 1.592 (Weast, 1978) and the viscosity of water (η_o) at 20°C is 0.01002×10^{-9} Nm^2S (Nobel, 1974), η for nonacclimated protoplasts was estimated to be 0.01280×10^{-9} Nm^2S and η for cold-acclimated protoplasts was estimated to be 0.01595×10^{-9} Nm^2S. To estimate ε_e it was again assumed that sorbitol and glucose have similar effects. A 0.5 M glucose solution has a relative dielectric constant, ε_{re} of approximately 68, and a 0.9 M glucose solution has an ε_{re} of approximately 62 (Washburn, 1928). Thus ε_e was estimated to be 6.02×10^{-10} F/m for nonacclimated protoplasts and 5.49×10^{-10} F/m for cold-acclimated protoplasts. After correcting for field weakening by adjacent electrodes and allowing for the field gradient ("error") within the central 10% of the distance between the electrodes, as shown in Appendix B, E was calculated to be $(6.25 \pm 2.4)\ 10^4$ V/m. Also in Eq. (9a) we assume $g_v g_f \approx 1$. With these estimates for the parameters of Eq. (9a), the maximum rate of protoplast rotation was calculated to be 1.10 ± 0.43 rad sec^{-1} for nonacclimated protoplasts and 0.81 ± 0.31 rad sec^{-1} for cold-acclimated protoplasts. The measured maximum rates of protoplast rotation (Table) although within the calculated ranges appear to be systematically smaller than the theoretical estimates. This may be due to the fact that $g_v g_f \neq 1$ or to other factors considered in the Discussion section.

The optimum frequency for protoplast rotation is linearly related to σ_e (Fig. 4). Because the intercept of the line is not significantly different from zero, for either nonacclimated or cold-acclimated protoplasts, the first term of Eq. (10) is effectively zero; therefore, R_m must be large ($R_m \gg 2$ MΩ). With a slope of 0.38 ± 0.03 (Fig. 4) and an average protoplast radius of 15.9 ± 0.1 μm (Table) the plasma membrane of nonacclimated protoplasts is calculated to have a specific capacitance of $(0.53 \pm 0.05) \times 10^{-2}$ F/m^2. (Note that R_m and C_m in Eq. (10) are the protoplast resistance and capacitance, respectively; the specific capacitance c_m is obtained by dividing C_m by the protoplast surface area; the specific resistance r_m is obtained by multiplying R_m by the protoplast surface area.) From the slope of 0.38 ± 0.03 (from Fig. 4) and the average protoplast radius of 14.2 ± 0.1 μm (Table), the specific capaci-

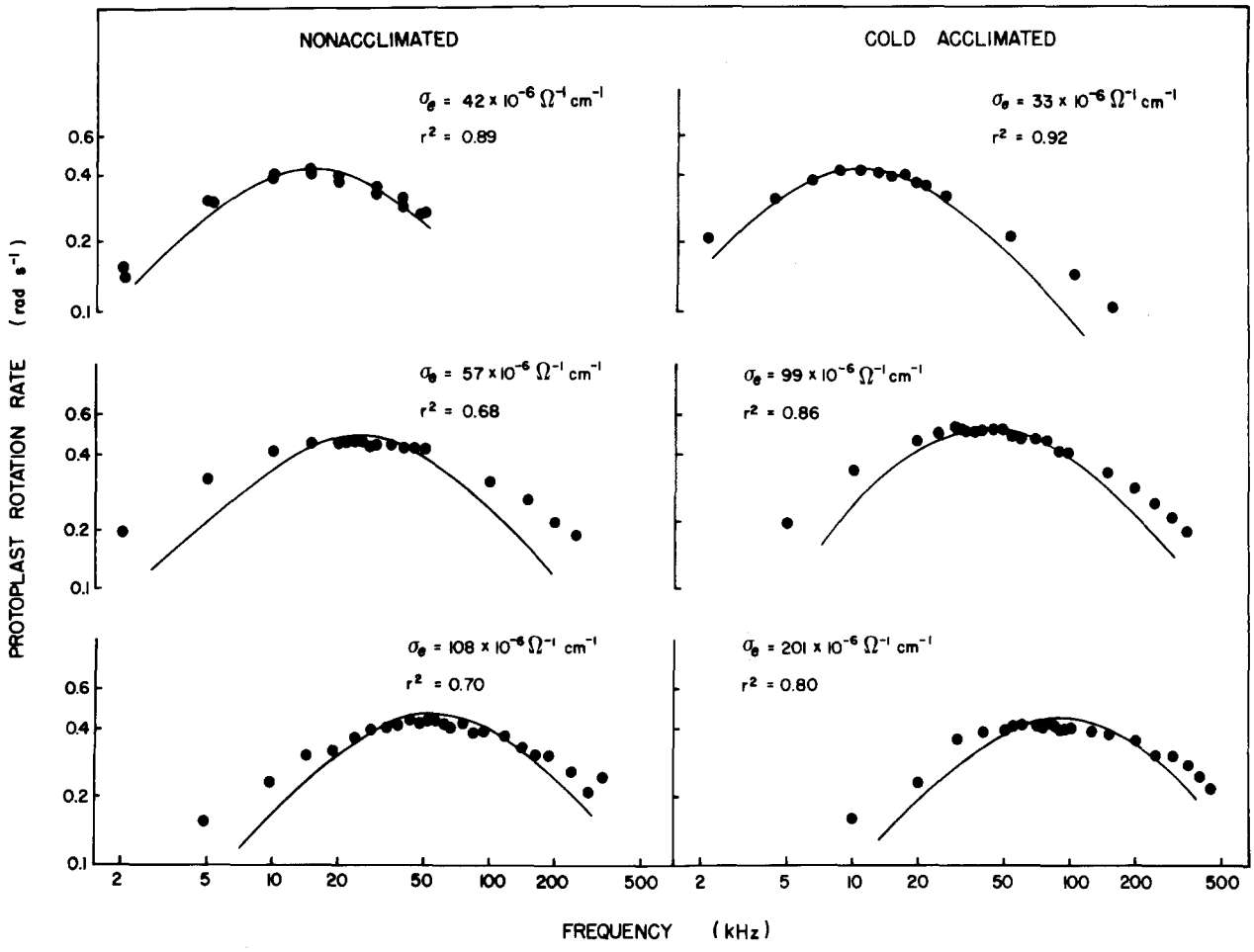

Fig. 3. Protoplast rotation rate as a function of the frequency of the electric field. Typical results for nonacclimated and cold-acclimated protoplasts at different values of σ_e are shown. Symbols are experimental data, and the solid line is the least-square fit (using an iterative procedure) to an equation with the form of Eq. (9a). The coefficient of determination (r^2) from the least-squares fit is shown. Notice that $10^{-6}\ \Omega^{-1}\ cm^{-1} = 10^{-4}\ \Omega^{-1}\ m^{-1}$

tance of the plasma membrane of cold-acclimated protoplasts is calculated to be $c_m = (0.59 \pm 0.05) \times 10^{-2}$ F/m^2.

Discussion

There is generally good agreement between the measured values (Figs. 3 and 4; and Table) and the values predicted by Eq. (9a) with $D = 1$. This agreement supports the validity of Eq. (9a) as derived in the Theory section, as opposed to the equation reported in the literature (Arnold & Zimmermann, 1982). The deviation of the experimental data from the model at high and low frequencies suggests that factors additional to those discussed in the Theory section may influence the cell rotation. Even though the measured maximum rate of protoplast rotation is within the range expected from the estimated variation of the electric field, the average measured rate is systematically lower than the predicted average rate by a factor of about 0.6. One possible factor contributing to give lower experimental values is that the electric field is actually smaller than predicted owing to weakening by surrounding metal of the microscope. A second possible factor is that $g_v g_f$ in Eq. (9a) is appreciably different from unity. In fact, the entire systematic difference between the measured and predicted values of $d\theta_c/dt$ can be accounted for if $g_v g_f \approx 1.67$. Using the estimate of $g_v \leq 1.22$ from Appendix C, this suggests a value of $g_f \approx 1.37$ for the friction factor. Further precision measurements are needed in order to distinguish between the influence of field weakening, friction and other factors.

When considering the possible role of R_m in ro-

tation studies it is useful to consider Eqs. (9a) and (11) as well as Eq. (10). For example, to determine if R_m influences the rotation, Eq. (10) may be used, and a plot of f_* versus σ_e may be made. For this, it is necessary that σ_e be precisely known. However, if one plots the maximum cell rotation rate as a function of σ_e, it is possible to search for a dependence of D on R_e. With this plot, a possible influence of R_m can be evaluated even if there is a fairly large uncertainty in the values of σ_e. It is important that both plots give a consistent conclusion regarding R_m.

Elodea canadensis cells have a specific plasma membrane resistance of 0.32 Ωm^2 and a specific tonoplast resistance of 0.058 Ωm^2 (Spanswick, 1972). *Avena sativa* coleoptile cells have a total specific resistance of 0.2 Ωm^2 (Etherton, Keifer & Spanswick, 1977). Using a value of 0.2 Ωm^2 and the value of 0.59×10^{-2} F/m^2, Eq. (10) predicts an intercept of 0.13 kHz. Inspection of Fig. 4 suggests that such a small intercept cannot be resolved. In fact, only a specific membrane resistance on the order of 0.004 Ωm^2, which corresponds to an intercept of 6.7 kHz, or larger could be resolved (*see also* Zimmermann & Arnold, 1983). Thus, the rotation method in its present form is not useful for measuring R_m of plant cells which have values of the specific membrane resistance and capacitance that are typical of higher plant cell membranes.

The values of $c_m = 0.53 \times 10^{-2}$ F/m^2 (nonacclimated) and 0.59×10^{-2} F/m^2 (acclimated) for the specific membrane capacitance, which we find for rye protoplasts, are similar to the value 0.48×10^{-2} F/m^2 found for *Avena sativa* protoplasts (Arnold & Zimmermann, 1982; *see also* Glaser, Fuhr & Gimsa, 1983). In contrast with the view that this capacitance results from the tonoplast and plasma membranes in series (Arnold & Zimmermann, 1982), we believe that the measured capacitance is mainly a property of the plasma membrane (*see* Appendix B). Thus, the present protoplast rotation studies give a specific membrane capacitance somewhat below the value of 10^{-2} F/m^2 considered typical of living cells (Zimmermann, 1982).

The plasma membrane plays a central role in the behavior of a cell during a freeze-thaw cycle, and destabilization of the plasma membrane is a primary cause of freezing injury (Steponkus, 1984). Because the freezing of electrolyte solutions is known to give rise to large steady and transient potential differences between the liquid and solid phases (Workman & Reynolds, 1950), electrically induced alterations of the plasma membrane may contribute to cryoinjury (Steponkus & Stout, 1983). Observations that protoplasts isolated from nonacclimated rye leaves lyse at lower applied electric fields than protoplasts isolated from cold-acclimated leaves are consistent with this possibility (Steponkus & Stout, 1983). Because there are no large changes in the electrical capacitance of the plasma membrane following cold acclimation, the increased stability of acclimated protoplasts is not attributable to differences in the charging time.

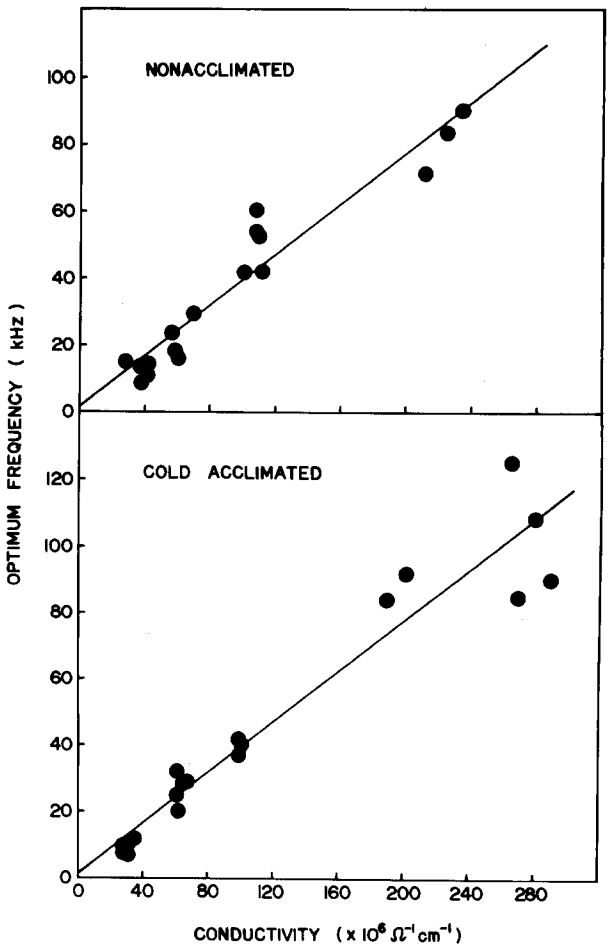

Fig. 4. Electric field frequency (f_*) causing maximum rate of protoplast rotation as a function of σ_e. f_* was determined by fitting experimental data, as shown in Fig. 1, to an equation with the form of Eq. (9a). The solid lines plotted were determined by least-square regression analysis. The regression analysis gave an intercept of 1.34 ± 3.38 (SE), a slope of 0.38 ± 0.03, and an r of 0.959 for nonacclimated protoplasts. For cold-acclimated protoplasts the intercept is 0.94 ± 3.97, the slope is 0.38 ± 0.03, and r is 0.962

The authors wish to thank Dr. R.M. Cotts for discussions that led to the use of a rotating electrical field, for direction in setting up the electrical apparatus, and for reviewing the manuscript. The authors thank W.W. Webb and R. Spanswick for a number of valuable discussions, and M. Oppenheim for valuable assistance with Appendix C. The able assistance of C.G. Fogelin in writing the software for ROTOPROTO and T.N. Björkman in determining K^+ concentrations is gratefully acknowledged.

This material is, in part, based on work supported by the National Science Foundation under Grant PCM-8021688 and the U.S. Department of Energy under Contract DE-AC02-81ER10917; Department of Agronomy Series Paper No. 1493.

References

Arnold, W.M., Zimmermann, U. 1982. Rotating-field induced rotation and measurement of the membrane capacitance of single mesophyll cells of *Avena sativa*. *Z. Naturforsch.* **37**:908–915

Batchelor, G.K. 1967. Fluid Dynamics. Cambridge University Press, Cambridge, p. 227

Coster, H.G.L., Smith, J.R. 1977. Low frequency impedance of *Chara corallina:* Simultaneous measurements of the separate plasmalemma and tonoplast capacitance and conductance. *Aust. J. Plant Physiol.* **4**:667–674

Etherton, B., Kiefer, D.W., Spanswick, R.M. 1977. Comparison of three methods for measuring electrical resistances of plant cell membranes. *Plant Physiol.* **60**:684–688

Furedi, A.A., Ahad, J. 1964. Effects of high-frequency electric fields on the living cell. I. Behavior of human erythrocytes in high-frequency electric fields and its relation to their age. *Biochim. Biophys. Acta* **79**:1–8

Glaser, R., Fuhr, G., Gimsa, J. 1983. Rotation of erythrocytes, plant cells, and protoplasts in an outside rotating electric field. *Stud. Biophys.* **96**:11–20

Holzapfel, C., Vienken, J., Zimmermann, U. 1982. Rotation of cells in an alternating electric field: Theory and experimental proof. *J. Membrane Biol.* **67**:13–26

Jackson, J.D. 1975. Classical Electrodynamics. John Wiley & Sons, New York

Landau, L.D., Lifshitz, E.M. 1959. Fluid Mechanics. Pergamon, London

Nobel, P.S. 1974. Introduction to Biophysical Plant Physiology. W.H. Freeman, San Francisco

Pohl, H.A., Crane, J.S. 1971. Dielectrophoresis of cells. *Biophys. J.* **11**:711–727

Simpson, R.E. 1974. Introductory Electronics for Scientists and Engineers. Allyn and Bacon, Boston

Spanswick, R.M. 1972. Electrical coupling between cells of higher plants: A direct demonstration of intercellular communication. *Planta* **102**:215–227

Steponkus, P.L. 1984. The role of the plasma membrane in freezing injury and cold acclimation. *Annu. Rev. Plant Physiol.* **35**:543–584

Steponkus, P.L., Dowgert, M.F., Ferguson, J.R., Levin, R.L. 1984. Cryomicroscopy of isolated protoplasts. *Cryobiology* **21**:209–233

Steponkus, P.L., Stout, D.G. 1983. Cryoinjury of isolated protoplasts: Possible involvement of electrical perturbations of the plasma membrane. *Cryobiology* **20**:727

Teixeira-Pinto, A.A., Nejelski, L.L., Cutler, J.L., Heller, J.H. 1960. The behavior of unicellular organisms in an electromagnetic field. *Exp. Cell Res.* **20**:548–564

Washburn, E.W. 1928. International Critical Tables of Numerical Data, Physics, Chemistry and Technology, Vol. 6. McGraw-Hill, New York

Weast, R.C. 1978. Handbook of Chemistry and Physics. Chemical Rubber Company, Cleveland, Ohio

Wiest, P.L., Steponkus, P.L. 1978. Freeze-thaw injury to isolated spinach protoplasts and its simulation at above freezing temperatures. *Plant Physiol.* **62**:699–705

Workman, E.J., Reynolds, S.E. 1950. Electrical phenomena occurring during the freezing of dilute aqueous solutions and their possible relationship to thunderstorm activity. *Phys. Rev.* **78**:254–259

Zimmermann, U. 1982. Electric field-mediated fusion and related electrical phenomena. *Biochim. Biophys. Acta* **694**:227–277

Zimmermann, U., Arnold, W.M. 1983. The interpretation use of the rotation of biological cells. *In* Coherent Excitations in Biological Systems. H. Frohlich and C. Kremer, editors. Springer-Verlag, Berlin

Received 14 February 1984; revised 11 June 1984

Appendix

A. Generation of Rotating Electric Fields

Figure 1 shows the geometry of the rotating-field chamber. Thin conducting plates (of platinum) are located at $x = L/2$, $-L/2 < y < L/2$ (plate #1); $y = L/2$, $-L/2 < x < L/2$ (#2); $x = L/2$, $-L/2 < y < L/2$ (#3), and $y = L/2$, $-L/2 < x < L/2$ (#4). The thickness of the conducting medium ($h \cong 200\ \mu$m) is fixed by horizontal glass plates and is much less than the separation of the plates, $L = 0.2$ cm. Therefore, the current density $\boldsymbol{J}$ and the electric field $\boldsymbol{E}_o$ in the chamber are essentially two-dimensional: $\boldsymbol{J} = \hat{x}J_x + \hat{y}J_y$ and $\boldsymbol{E}_o = \hat{x}E_x + \hat{y}E_y$. Ohm's law implies $\nabla \cdot \boldsymbol{J} = 0$ or $\nabla \cdot (\sigma_e \boldsymbol{E}_o) = 0$ or $\nabla^2\Phi = 0$, where $\Phi(x,y)$ is the electrostatic potential with $\boldsymbol{E}_o = -\nabla\Phi$. The boundary conditions are simply that Φ be a constant on each plate. We consider two possible electrical configurations for driving the potentials on the four plates so as to give a rotating electric field at $x = 0$, $y = 0$.

The first configuration is symmetrical with $\Phi_1 = -(\Phi_o/2)\sin(\omega t)$, $\Phi_2 = (\Phi_o/2)\cos(\omega t)$, $\Phi_3 = (\Phi_o/2)\sin(\omega t)$, and $\Phi_4 = -(\Phi_o/2)\cos(\omega t)$, where Φ_o is the peak-to-peak applied voltage amplitude and $\Phi_1, \ldots, \Phi_4$ are the potentials on the plates, and ω is the angular frequency of the external signal generator. It is clear that the electrostatic potential can be derived at $t = 0$ and at $t = \pi/(2\omega)$, and that a superposition of these two potentials will give the potential at an arbitrary instant of time. The potential at $t = \pi/(2\omega)$ can be obtained from the potential at $t = 0$ by replacing x by $-y$ and y by x. Superposition then gives

$$\Phi(x,y,t) = \cos(\omega t)\Phi(x,y,t=0) - \sin(\omega t)\Phi(-y,x,t=0). \qquad \text{(A1)}$$

At $t = 0$, we find

$$\Phi(x,y,t=0) = \Phi_o \sum_{m=1,3,5\ldots} \frac{2(-1)^{\frac{m-1}{2}}}{m} \frac{\cos(m\pi x/L)\sinh(m\pi y/L)}{\sinh(m\pi/2)}. \qquad \text{(A2)}$$

Near the center of the chamber, the Taylor expansion of Eq. (A2) gives

$$\Phi(x,y,0) = (\Phi_o/L)\left\{c_1 y - \left[\frac{c_3}{2L^2}\right]\left[x^2 y - \frac{y^3}{3}\right] + \ldots\right\} \qquad \text{(A3)}$$

where $c_1 \cong 0.8346$ and $c_3 \cong 5.7382$. From Eq. (A1), the leading term proportional to c_1 is seen to give a uniformly rotating electric field of magnitude equal to $c_1(\Phi_o/L)$. The constant c_1 provides

a correction for field weakening caused by the adjacent metal electrodes. The rotation rate of the field is ω.

The cubic term in Eq. (A3) gives an "error" contribution to the electric field. A dimensionless measure of the influence of this error field on the cell rotation is given by

$$\varepsilon \equiv (\boldsymbol{E})^2 \left(\frac{c_1\Phi_0}{L}\right)^{-1} - 1 \lesssim \frac{2c_3}{c_1}\left(\frac{r}{L}\right)^2, \tag{A4}$$

where $r^2 = x^2 + y^2$. For example, to have $\varepsilon < 0.1$ we need $r/L < 0.085$.

The second configuration is asymmetrical and has $\Phi_1 = -(\Phi_o/2)\sin(\omega t)$, $\Phi_2 = (\Phi_o/2)\cos(\omega t)$, $\Phi_3 = 0$, and $\Phi_4 = 0$, where Φ_o is again the peak-to-peak amplitude of the signal generator. At $t = 0$ we find

$$\Phi(x,y,t=0) = \frac{\Phi_o}{2}\sum_{m=1,3,5\ldots} \frac{4(-1)^{\frac{m-1}{2}}}{m\pi} \frac{\cos\left(\frac{m\pi x}{L}\right)\sin\left(\frac{m\pi}{2} + \frac{m\pi y}{L}\right)}{\sinh(m\pi)}. \tag{A5}$$

Equation (A1) also applies in this case. Near the center of the chamber, the expansion of Eq. (A5) gives

$$\Phi(x,y,t=0) = (\Phi_o/2)[c_o + c_1(y/L) - c_2(x^2 - y^2)/L^2 \ldots] \tag{A6}$$

where $c_o = 0.25$, $c_1 = 0.8346$, and $c_2 \cong 1.9042$. The leading term proportional to c_1 is again seen to give a rotating electric field of constant magnitude $c_1\,\Phi_o/(2L)$ with constant rotation rate ω.

The quadradic terms in Eq. (A6) give rise to an "error" in the field. A measure of this error is

$$\varepsilon \equiv (\boldsymbol{E})^2 \left(\frac{c_1\Phi_o}{2L}\right)^{-2} - 1 \lesssim \frac{6c_2}{c_1}\left(\frac{r}{L}\right). \tag{A7}$$

In order to have $\varepsilon < 0.1$, we need in this case to have $r/L < 0.013$. This limitation on r/L is more restrictive than that for the symmetric case [Eq. (A4)]. However, an advantage of the asymmetrical configuration is the simplicity of the required driving voltages.

An estimate of the resistance of the chamber, say, between the #2 and #4 plates is easily found to be $[4\sigma_e h \ln(L/\delta L)]^{-1}$, where δL is the gap distance between plate corners.

B. Polarizability of a Spherical Cell

The assumed cell geometry is shown in Fig. 2. The uniform, but time-dependent, external electric field has an electrostatic potential

$$\Phi_o = -rE_o(t)\cos\theta,$$

where a spherical (r,θ,ϕ) coordinate system centered on the cell is used. In the separate regions—inside the cell, outside the cell, and within the membrane—we have $\nabla \cdot \boldsymbol{J} = 0$ or $\nabla \cdot (\sigma \boldsymbol{E}) = \sigma\nabla^2\Phi = 0$, where $\boldsymbol{J}$ is the current density. Thus, the induced potential is everywhere proportional to the first Legendre polynomial $P_1(\cos\theta) = \cos(\theta)$. Inside the cell, $\Phi_i = K_i r\cos\theta$; within the membrane $\Phi_m = (K_m r + K'_m r^{-2})\cos\theta$; and outside the cell $\Phi_e = -rE_o\cos\theta + (K_e/r^2)\cos\theta$. Hence, there are four constants, K_i, K_m, K'_m, and K_e, to be determined.

At each interface, there are two jump conditions on Φ. One condition follows from the continuity of the tangential component of $\boldsymbol{E}$. The second condition follows from the continuity equation, which gives $[\sigma E_r] = i\omega\Sigma_f$, with $[\ldots]$ denoting the difference of the outer and inner values, and Σ_f the free surface charge density at the interface, and Poisson's equation which gives $[\varepsilon E_r] = \Sigma_f$. Thus, four equations result from the conditions at the two interfaces:

$$K_i = K_m + K'_m/(r_a)^3, \tag{B1/a}$$

$$(\sigma_m - i\omega\varepsilon_m)[K_m - 2K'_m/(r_a)^3] = (\sigma_i - i\omega\varepsilon_i)K_i, \tag{B1/b}$$

$$-E_o + K_e/(r_b)^3 = K_m + K'_m/(r_b)^3, \tag{B1/c}$$

$$(\sigma_e - i\omega\varepsilon_e)\left(E_o + \frac{2K_e}{(r_b)^3}\right) = (\sigma_m - i\omega\varepsilon_m)\left(-K_m + \frac{2K'_m}{(r_b)^3}\right). \tag{B1/d}$$

The actual physical quantities are taken to be the real parts of the complex quantities which have time dependencies of the form $\exp(-i\omega t)$.

Equations (B1) can be solved to give the K's in terms of E_o. In particular, for $\sigma_e \gg \omega\varepsilon_e$, $\sigma_i \gg \omega\varepsilon_i$, and $\bar{r} \gg \delta$, we find

$$K_e = -(\bar{r})^3 E_o \frac{\sigma_e - \sigma_i + \frac{\delta}{\bar{r}}\frac{\sigma_e\sigma_i}{(\sigma_m - i\omega\varepsilon_m)}}{2\sigma_e + \sigma_i + 2\frac{\delta}{\bar{r}}\frac{\sigma_e\sigma_i}{(\sigma_m - i\omega\varepsilon_m)}}. \tag{B2}$$

From Eq. (4) of the Theory section, the electric dipole moment of the protoplast is $\boldsymbol{p} = \alpha\boldsymbol{E}_o$, where the polarizability is

$$\alpha = 4\pi\varepsilon_e K_e/E_o. \tag{B3}$$

Equations (6), (B2), and (B3) can be combined to give Eq. (7). Notice that for $\sigma_m = 0$ and $\omega \to 0$, we have $\alpha = -2\pi\varepsilon_e(\bar{r})^3$. The fact that α is negative in this limit is due to the exclusion of the $\boldsymbol{E}$ field lines (or equivalently current-density lines) from the inside of the sphere. This induced dipole moment has the opposite sign to that which would be induced on, say, a single isolated molecule in vacuo.

With the same approximations as used to obtain Eq. (B2), the potential drop across the membrane is found to be

$$\delta\Phi_m = \Phi_e(r_b) - \Phi_i(r_a) = \frac{-3E_o\delta}{(1 + 2\sigma_e/\sigma_i)(\sigma_m - i\omega\varepsilon_m)/\sigma_e + 2(\delta/r)}. \tag{B4}$$

The electric field inside the protoplast is uniform with a magnitude

$$E_i = \frac{3(\sigma_e/\sigma_i)E_o(\sigma_m - i\omega\varepsilon_m)/\sigma_e}{(1 + 2\sigma_e/\sigma_i)(\sigma_m - i\omega\varepsilon_m)/\sigma_e + 2(\delta/r)}. \tag{B5}$$

For the experimental conditions, $\sigma_i \gg \sigma_e$, $(\sigma_i/\sigma_e > 38)$ and, consequently, $E_i \ll E_o$. That is, the inside of the protoplast is essentially an equipotential. We estimate that the influence of the vacuole is at most (perfect insulation) to reduce the effective value of σ_i by a factor of the order of the two-thirds power of the volume fraction of the vacuole. From direct microscopic observations we estimate that this factor is of the order of 0.5. [The vacuole usually appears to be asymmetrically situated inside the protoplast with the vacuole apparently in close contact with the plasma membrane over a small fraction (<0.2) of the surface area of the protoplast. This small region of possibly close contact does not alter the conclusion that the cytoplasm is essentially an equipotential.] Even with this reduction of σ_i the cytoplasm of

the protoplast will be an equipotential. Notice also that Eqs. (B2)–(B5) are independent of σ_i for $\sigma_i \gg \sigma_e$.

For $\sigma_i \gg \sigma_e$, Eqs. (B2)–(B5) may be understood qualitatively in terms of a simple lumped parameter model: The membrane is represented as a resistor $R_m = \delta[4\pi(\bar{r})^2\sigma_m]^{-1}$ in parallel with a capacitor $C_m = 4\pi(\bar{r})^2\varepsilon_m\delta^{-1}$. The membrane is in turn connected in series to a resistor $R_e = [4\pi\bar{r}\sigma_e]^{-1}$, which represents the external medium. The external voltage, $\sim E_o\bar{r}$, is applied across the series circuit. For example, the voltage across the membrane in the lumped parameter model is $Z_m[Z_m + R_e]^{-1}[E_o\bar{r}]$, where $Z_m = [R_m^{-1} + \omega C_m/i]^{-1}$ is the membrane impedance. This expression for $\delta\Phi_m$ is of the form of Eq. (B3), but without the correct numerical coefficients.

C. Viscous Drag on a Rotating Sphere which Rests on a Plane Surface

The evaluation of the drag force on a uniformly rotating solid sphere in an infinite viscous medium is discussed by Landau and Lifshitz (1959). However, for the experimental conditions of interest the sphere rests on a horizontal (x, y) plane while rotating about the z-axis. For such conditions the drag force can be obtained using Helmholtz's minimum energy dissipation theorem (Batchelor, 1967). This theorem states simply that the actual Stokes' flow is the unique flow which (i) satisfies no slip boundary conditions on the sphere and the horizontal surface and (ii) gives a minimum of the viscous energy dissipation in the fluid.

Without loss of a generality we write the fluid velocity as $v = \phi\Omega r \sin\theta$, where a spherical (r, θ, ϕ) coordinate system is used (with $r = 0$ the center of the sphere, and $r = \bar{r}$ and $\theta = 0$ the point of contact of the sphere and the horizontal surface), and where $\Omega = \Omega(\bar{r},\theta)$. This no-slip boundary condition on the sphere is $\Omega(\bar{r},\theta) = \Omega_o = d\theta_c/dt = \text{const.}$, whereas the no-slip condition on the horizontal surface is $\Omega(r/\cos\theta, \theta) = 0$ for $0 \le \theta \le \pi/2$. The viscous energy dissipation rate can be expressed as

$$\dot{W}(\Omega) = \eta \int_{\text{fluid}} 2\pi r^2 \sin\theta dr d\theta (\sin\theta)^2 \left[\left(\frac{\partial\Omega}{\partial\theta}\right)^2 + r^2\left(\frac{\partial\Omega}{\partial r}\right)^2\right]. \quad \text{(C1)}$$

Helmholtz's theorem states that the actual flow, $\Omega(r,\theta)$, is that flow which minimizes $\dot{W}$ while satisfying the boundary conditions. The drag torque on the sphere is then simply

$$N_z^v = -\min(\dot{W})/\Omega_o. \quad \text{(C2)}$$

Any function $\Omega'(r,\theta)$ other than the actual flow which satisfies the boundary conditions will give $\dot{W}(\Omega') \ge \min[\dot{W}(\Omega)]$. Therefore, we may use a trial function in Eqs. (C1) and (C2) to obtain an upper bound on the torque. A convenient choice for the trial function is

$$\Omega'(r,\theta) = \Omega_o(\bar{r}/r)^3\left[1 - \left(\frac{r}{\bar{r}} - 1\right)\left(\frac{1}{\mu} - 1\right)^{-1}\right], \quad \text{(C3a)}$$

for $0 \le \theta \le \pi/2$, and

$$\Omega'(r,\theta) = \Omega_o(\bar{r}/r)^3, \quad \text{(C3b)}$$

for $\pi/2 < \theta \le \pi$. This function satisfies the boundary conditions. A direct evaluation of Eq. (C1) gives

$$\dot{W}(\Omega') = 8\pi\eta(\bar{r})^3\Omega_o^2[\tfrac{11}{9}]. \quad \text{(C4)}$$

Therefore, if we express the actual drag torque as

$$N_z^v = -8\pi g_v \eta(\bar{r})^3\Omega_o, \quad \text{(C5)}$$

then equation (C4) and Helmholtz's theorem imply that

$$g_v \le \tfrac{11}{9} = 1.222\ldots. \quad \text{(C6)}$$

Equivalently, we conclude that the drag force is increased by *less* than 22% as compared with the case of a sphere in an infinite fluid.